

RESEARCH ARTICLE

Poly-L-Lysine Inhibits Tumor Angiogenesis and Induces Apoptosis in Ehrlich Ascites Carcinoma and in Sarcoma S-180 Tumor

Souvik Debnath¹, Saumen Karan¹, Manish Debnath², Jyotirmayee Dash², Tapan Kumar Chatterjee^{1*}

Abstract

Background: This study focuses on the role of Poly-L-lysine (PLL), an essential amino acid, on molecular changes of tumor angiogenesis suppression, pro-apoptotic and anti-apoptotic gene expression after treatment on Ehrlich ascites carcinoma (EAC) and solid sarcoma-180 tumor cells bearing mice. **Materials and Methods:** The cell viability was carried out using MTT assay. The antitumor activity was evaluated by treatment with PLL at 20 and 40mg/kg/b.w doses for 14 days in EAC ascites tumor and 21 days for Sarcoma-180 solid tumor model. Several tumor evaluation studies, haematological and biochemical parameters were estimated. Importantly, the tumor cell apoptosis was assessed using microscopic observations, DNA fragmentation assay, Flow cytometric analysis, cell-cycle and electron-microscopic study, following which, the expression of several signal proteins related to pro-apoptosis, anti-apoptosis and tumor angiogenesis were quantified using western blotting and immunohistochemistry study. **Results:** Precisely, PLL had cytotoxic effect on K562; A549; U937 and B16F10 cancer cells. Significant decreases in liquid and solid tumors and increased life span of treated mice were observed ($P < 0.05$). Typical morphological changes, apoptosis bleb phenomenon and sub-G₁ cell cycle arrests revealed that PLL promoted apoptotic cell death. Western blot and immunohistochemistry confirms, PLL activated apoptotic signalling cascades through down regulation of Bcl-2 and CD31 protein and up-regulation of Bax and p53 proteins. The anti-angiogenic effects were also accompanied with decreased VEGF expression and reduced peritoneal-angiogenesis and microvessel density. **Conclusions:** The antitumor and antitumor-angiogenic activity of PLL was confirmed from all the results via up and down regulation of relevant signal proteins reported in this publication.

Keywords: Pro-apoptosis- anti-apoptosis- anti-angiogenesis- cell viability- DNA fragmentation- micro vessel density

Asian Pac J Cancer Prev, **18** (8), 2255-2268

Introduction

Despite advances in medical research and remarkable strides to facilitate cancer treatment, it is still the cause of the second highest mortality rate after cardiovascular diseases, worldwide (Torre et al., 2015). Development of tumor resistance against the available treatment modes together with patient noncompliance invokes the requirements for safe, newer drugs and extensive research on synthetic drug molecules for cancer treatments.

It is well known that tumor growth and metastasis depend on angiogenesis and lymph angiogenesis triggered by chemical signals from tumor cells in a phase of rapid growth (Ferrara et al., 2003; Folkman et al., 1971). The process of angiogenesis comprises complex and diverse cellular actions such as extracellular matrix degradation, proliferation, migration and morphological differentiation of endothelial cells to form tubes (Carmeliet et al., 2000).

Inhibiting tumor angiogenesis may halt tumor growth and decrease their metastatic potential. The cytokine vascular endothelial growth factor (VEGF) is the most important angiogenic factor associated closely with induction and maintenance of neovasculature structure in tumor (Bussolino et al., 1997; McMahon et al., 2000), so the inhibition of VEGF expression is known to have an impact on angiogenesis dependent tumor growth and metastasis.

The role of apoptosis and the genes that control it in cancer have a profound effect on the malignant phenotype. It has now been revealed that oncogenic mutations disrupt apoptosis, leading to tumor initiation, progression or metastasis. Conversely, compelling evidence indicates that other oncogenic changes promote apoptosis, thereby producing selective pressure to override apoptosis during multistage carcinogenesis (Lowe et al., 2000). It has been established that Bcl-2-family proteins play central roles in cell death regulation and are capable of

¹Pharmacology Laboratory, Department of Pharmaceutical Technology, Jadavpur University, Jadavpur; ²Department of Organic Chemistry, Indian Association for the Cultivation of Science, Jadavpur, Kolkata, India. *For Correspondence: crctkc@gmail.com

regulating diverse cell death mechanisms that encompass apoptosis, necrosis and autophagy (Cory et al., 2003; Yip et al., 2008). Alterations in their expression and function contribute to the pathogenesis and progression of human cancers, thus providing targets for drug discovery the members of Bcl-2 family which can be classified into two groups, anti-apoptotic and pro-apoptotic and they form heterodimers to inactivate each other. The up-regulation of Bax expression and the down regulation of Bcl-2 at protein level have been demonstrated during apoptosis (Reed et al., 2000). Among the positive and negative regulators of apoptosis, p53 tumor suppressor gene has an important role against cancer as it suppresses tumor growth through, cell cycle arrest and apoptosis (Das et al., 1999). The underlying mechanism as above can be understood following the changes in p53 expression (Donati et al., 2012). Bax, the pro-apoptotic member of Bcl-2 family, is a p53 target and is trans-activated in a number of systems during p53 mediated apoptosis (Toshiyuki et al., 1995; Guo et al., 2016).

For many years now, poly-L-lysine, PLL, has been known to have unusual biological properties, an early report indicating that PLL has some activity against murine tumors. Being cationic in nature, it permeates cancer cells through the cell membrane. Among the D and L-isomers of the same, the latter is much more effective in inhibiting cell growth by tightly binding to the cell membrane (Arnold et al., 1979). Early studies have shown that inhibits the tobacco mosaic virus (Stahmann et al., 1951), blocks the development of bacteriophage (Watson et al., 1952), possesses antibacterial activity and protects chicken embryos from animal viruses (Bichowsky - Slomnicki et al., 1956). An early report indicates that PLL has some activity against murine tumors (Green et al., 1953), and increases the transport of specific radioisotopes into cells (Anghileri et al., 1976). Additionally, PLL exhibits enhanced antitumor actions as a carrier of anticancer drugs, when applied to HeLa and L1210 murine leukemia cells (Arnold et al., 1978). The biological investigation of this compound shows retardation of cell proliferation, in the *in-vivo* tumor models without any toxic side effects (Szende et al., 2002).

Ehrlich ascites carcinoma (EAC) is a spontaneous, undifferentiated, murine mammary adeno-carcinoma cell line, hyperdiploid in nature, has high transplantable capability, rapid proliferation, shorter life span, 100% malignancy and does not have tumor specific H-2 histocompatibility transplantation antigens (Chen et al., 1970). This is the primary reason for its rapid proliferation in any mouse host (Patt et al., 1956). Whereas, sarcoma-180 is a malignant, heterogeneous, mouse tumor cell line of mesodermal origin and its growth is observed in a wide range of pulmonary metastasis among inbred mouse strains (Lee et al., 2003; Britto et al., 2012).

The precise anti-tumorigenic and anti-angiogenic mechanism of PLL in Ehrlich ascites carcinoma and Sarcoma-180 solid tumor cells remains unknown still. In the present communication, we demonstrate the efficacy of the PLL amino acid on murine mammary Ehrlich ascites tumor (liquid tumour) and sarcoma-180 (solid tumor) cell lines at the molecular level to demonstrate its potential

anti-tumor, apoptosis and angio-preventive activities.

Materials and Methods

Chemicals and Reagents

PLL hydrobromide (Mrs 30,000 – 70,000) and 3-(4, 5-Dimethylthiazol-2-yl) –2, 5-diphenyltetrazolium bromide (MTT) was obtained from Sigma-Aldrich (USA). Giemsa stain, Haematoxylin and Eosin stain, Papanicolaou stain were obtained from Qualigene (Mumbai, India). Cell cycle reagent was purchased from Merck Millipore (USA). Terminal deoxynucleotidyltransferase-mediated dUTP nick end labeling kits were from BD Bioscience (USA), Propidium Iodide (PI), acridine orange, 4',6 – diamidino-2-phenyl indole (DAPI) were purchased from Sigma Chemical Co. (St. Louis, USA). Genomic DNA purification kit was purchased from Fermentas (USA). Annexin V and primary antibodies were obtained from BD Bioscience (USA). Secondary anti-bodies were purchased from Sigma (USA). Dulbecco's modified Eagle medium (DMEM), Penicillin, streptomycin and neomycin (PSN), fetal bovine serum (FBS), trypsin and ethylene di-amine tetra-acetic acid (EDTA), Trypan blue were obtained from HiMedia (India). A primary antibody for immunohistochemistry study CD31 was obtained from Santa Cruz Biotechnol. Inc., CA USA. Bcl-2 antibody was purchased from Anaspec, USA. p53 was purchased from Pathn Situ Biotechnologies, India.

Preparation of the drug solution

The solution of PLL was prepared by dissolving dry lyophilized PLL hydrobromide (Figure 1) in sterile phosphate buffered saline (PBS, pH: 7.4). For *in-vivo* studies, PLL solution was administered by intraperitoneal injections (i.p.) of 20 mg/kg b.w and 40 mg/kg b.w (Arnold et al., 1979). The solution was kept at 4°C to maintain stability for extended use.

Cell lines and cell culture

In-vitro cancer cell lines K562, A549, and U937 cancer cells were obtained from National Centre for Cell Science (NCCS), Pune, India and EAC, Sarcoma-180, B16F10 cancer cells were collected from Chittaranjan National Cancer Research Institute (CNCRI), Kolkata, India. The *in-vitro* cells were maintained in Dulbecco's modified Eagle's medium (DMEM), (HiMedia India) supplemented with 10% FBS at 37°C in CO₂ incubator

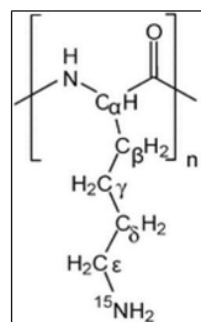


Figure 1. Poly-L-Lysine Hydrobromide (Mrs: 30,000-70,000)

in an atmosphere of humidified 5% CO₂ and 95% air. The cells were maintained routinely in subcultures in tissue culture flasks. The EAC, Sarcoma-180 and B16F10 cells were maintained in the peritoneal cavity of mice by injecting 0.1ml at fluid cell every 7 days. Tumor cell counts were done in a Neubauer hemocytometer using the trypan blue dye exclusion method. Cell viability was always found to be 95% or more (Sangameswaran et al., 2012). Tumor cell suspensions were prepared in phosphate buffered saline (PBS).

Animals

Eight to ten per cage of healthy inbred strains of Swiss female albino mice (*Mus musculus*) weighing about 20 gm were kept for at least 14 days in environmentally controlled room temperatures (23±2°C), humidity (50±5%) and light (12 hour light/ dark cycle) and were given food and water *ad libitum*. All experiments were conducted as per guidelines cleared by the Animal Ethics Committee of the Department of the Pharmaceutical Technology of Jadavpur University, India (Registration number: 147/1999/CPCSEA).

In-vitro experiment

MTT Assay

This test is based on MTT (3-(4, 5- dimethylthiazol-2-yl)-2, 5-diphenyl tetrazolium bromide), which is reduced to purple-blue soluble formazan by the living cells. Experiments were performed in 96-well flat bottomed culture plates (BD Biosciences, USA). MTT was dissolved in phosphate buffered saline (PBS) at a concentration of 5mg/ml. Next to this, different concentrations of PLL (0.1, 0.5, 1, 5, 10, 20, 20 µg/ml) were added and the plate was incubated for a period of 24 h. Following this, 20 µL of MTT solution, prepared as above, was added to each well and incubated for 4 h at 37 °C, the culture medium was removed, and the formazan crystals were dissolved in 200 µL DMSO. Absorbance of formazan dye was measured at 570 nm using a microplate reader (Tarsons, India, Cat. No: 980040). The percentage of viable cells was determined by the following equation:

$$\text{Viable cells (\%)} = \frac{A \text{ of treated cells}}{A \text{ of untreated cells}} \times 100$$

(Mosmann et al., 1983)

In-vivo experiment

Experimental Design

24 animals were divided into 4 groups (6 animals per group), e.g., group I, II, III, IV, respectively. Ascites fluid was drawn out from EAC tumor bearing mouse at the log phase (day 7-8 of tumor bearing) of the tumor cells. Each animal was inoculated with 0.1 ml of tumor cell suspension, prepared in phosphate buffer solution containing 2×10⁶ cells/ml. (Mosmann et al., 1983). Group-I was considered as an EAC control. After 24 h of EAC cell transplantation, group-II and III of the experimental animals received PLL at doses of 20 and 40 mg/kg b.w, i.p. respectively and the Group-IV received the reference drug, 5-FU (20 mg/kg i.p.), for 14 consecutive

days (Mizuno et al., 1999). After the last dose, the animals were fasted for a period of 18 h, followed by sacrifice by cervical dislocation. Ascitic fluid was collected for further study and inner lining of the peritoneal cavity was examined for peritoneal angiogenesis (Sreelatha et al., 2011).

In the case of sarcoma-180 solid tumor model 24 mice were divided into 4 groups (6 animals per group), group I, II, III, IV, respectively. Each group was given subcutaneous inoculation (s.c.) of 0.1 ml sarcoma-180 cell suspension containing 2×10⁶ cells/ml. Group-I served as the control, followed by treatments groups-II and III, receiving doses of (20 and 40 mg/kg of b.w) of PLL (i.p), respectively similar to as described for the liquid tumor model experiments described earlier. Treatment was started 10 days after tumor inoculations, and was continued for 21 days, similar to the solid tumor model (Ozaslan et al., 2011). The last group (group-IV) received the standard drug 5-FU. After experiment 21 days, animals were sacrificed through cervical dislocation, for additional studies.

EAC peritoneal tumor model

Tumor evaluation

After injecting EAC cells (2×10⁶ cells/ml) i.p. in mice the body weight of the mice was monitored from the 1st day till the 14th day. Animals were sacrificed on the 15th day, 2ml of saline water was injected (i.p.), and a small incision was made in the abdominal region to collect the tumor cells along with ascites fluid. Then EAC cells along with the ascites fluid were harvested into 15ml. centrifuge tubes and centrifuged at 3,000 rpm for 10 min at 4°C. The ascites fluid volume was measured by subtracting the volume of saline injected while harvesting the EAC cells from the total ascites fluid volume measured and the packed cell volume was determined. The pelleted viable and nonviable cells were counted by trypan blue dye exclusion method using a haemocytometer.

$$\text{Cell count} = \frac{(\text{Number of cells X dilution factor})}{(\text{Area X thickness of liquid film})}$$

Determination of mean survival time and percentage increase in life span

The animal survivals were recorded for up to 40 days. The tumor response was assessed on the basis of the mean survival time (MST) and percentage increase life span (%ILS). Mortality was monitored by recording (% ILS) and (MST) as per the following formula:

$$\% \text{ ILS} = \left[\frac{\text{Mean survival time of the treated group} - 1}{\text{Mean survival time of the control group}} \right] \times 100$$

(Gayatri,S., et al., 2015)

Mean survival time = (Day of first death + Day of last death) / 2 (Samudrala, et al. 2015). Here, the time is denoted by number of days.

Estimation of hematological and serum biochemical parameters

After 14 days from the outset of the experiment, animals were sacrificed by cervical dislocation and blood samples were collected from the heart using heparinized syringes for hematological and serum biochemical parameters.

Histopathology of liver tissue

Three randomly selected mice from each group were sacrificed and their liver tissues isolated. Post isolation from adhering tissue matter, the livers were washed with saline and weighed, cut into small pieces, fixed in 10% buffered formalin, dehydrated in increasing concentrations of ethanol, cleared in xylene and embedded in paraffin wax. Sections (5 to 6 μ m thick) were cut, stained with hematoxylin and eosin (H&E) and examined under a light microscope (Eclipse TS100, Nikon, Japan).

Study on change in morphology of EAC cells by staining method

EAC cells from the treated and control groups were centrifuged at 3000 r.p.m. for 10 min and were fixed on a glass slide in the neutral buffered formalin. The fixed samples were stained with hematoxylin and eosin. Another part of EAC cells from the treated and control groups were used for Papanicolaou staining. Slides were prepared from the samples collected from each group, using 95% ethanol for fixation, followed by staining the same with papanicalaou stain. Next to this, the slides were mounted with DPX (DistreneDibutylPthalate Xylene) and were examined under the light microscope (Eclipse TS100, Nikon, Japan).

Anti-angiogenic effects of the compounds in peritoneal angiogenesis

On day 15 post tumor inoculation, the skin peritoneum of the mice was cut to open the inner lining of the peritoneal cavity and examined for angiogenesis in control and test compound (Poly-L-lysine) treated tumor bearing mice and photographed.

Apoptotic analysis

Flow cytometry using Annexin-V/PI

In order to evaluate apoptosis, externalization of phosphatidylserine during apoptosis and leakage from necrotic cells was observed by annexin V-FITC/PI dual staining propidium iodide (PI, 0.5 μ g/mL) and Annexin V-FITC (25 μ g/mL) using standard protocol. The assay was performed according to the assay kit procedures (BD Biosciences, USA) and analysed by flow cytometer (model, make) within 1 hr.

TUNEL assay using flow cytometry

To confirm the nature of tumor killing by PLL, Terminal deoxynucleotidyltransferase – mediated dUTP Nick End Labeling (TUNEL) assay was performed. EAC cells were fixed, permeabilized and incubated with TdT enzyme and FITC-Br-dUTP. Cells were washed, incubated with PI/RNase solution and samples analyzed using flow cytometry.

DNA fragmentation assay

The collected EAC cells were washed twice using PBS and pelleted. The pelleted cells were lysed using 600 μ L of Lysis buffer (10 mM Tris-HCl buffer, PH 8.0, 10mM EDTA and 0.2% Triton X-100) for 10 min, kept in ice box. The lysate was centrifuged at 6000 rpm for 20 min. The supernatant was extracted with 1000 μ L of PCIAA (Phenol-Chloroform-Isoamyl alcohol solution, 25:24:1) and the mixture was centrifuged at 6000 rpm for 20 min. The upper layer was discarded, precipitated with 50 μ L of 3M NaCl and 1000 μ L of cold ethanol at 20°C overnight. Post overnight drying, isolated DNA was dissolved in TE buffer and incubated with 40 units of RNase solution to minimize possible RNA contaminations at 37°C for 30 min. Loading buffer was added and fragmented DNA electrophoresed on 2% agarose gel in TBE (40 mM Tris, 20mM Boric acid, 1mM EDTA) at 100 V for 45 min and visualized using EtBr staining on a Bio-Rad (USA) gel documentation system.

Fluorescence microscopy study

DAPI staining

Assessments of chromatin condensations and nuclear blebbing in EACs from tumor-bearing mice treated with and without PLL were fixed with methanol. The cells were stained with DAPI (1 μ g/ml for 15 min at room temperature). Apoptotic cells were observed using a Leica Germany Model DM900 fluorescent microscope.

Cell cycle analysis by flow cytometry

1 ml cell suspension was taken in a tube, centrifuged, supernatant discarded, 1 ml ammonium chloride red blood cell lysis buffer was added to the pellet, mixed gently, incubated for 2 – 5 min at 37° C for red blood cell lyses. After incubation cells were centrifuged, supernatant discarded, washed twice with 5 ml PBS, re-suspended in 3 ml ice cooled 70% ethanol and incubated for a period of 30 min in ice. After incubation, the centrifuged supernatant was discarded, 25 μ l RNase solution (1 mg/ml in PBS) was added, mixed and incubated for 30 min at room temperature. Then 50 mg/ml concentration of PI solution was added to the cells and incubated for 30 min at room temperature in the dark. After incubation the cells were mixed well and analysed using a flow cytometer.

Western blot analysis

EAC cells were harvested from control and drug treated mice. Cells were centrifuged and washed once with 1X PBS (pH 7.4) and lysed with cold cell lysis buffer (20 mM Tris, 100 mM NaCl, 1 mM EDTA in 0.5% Triton X-100). Cell lysates were collected and the total protein contents estimated by the Lowry method. The protein contents from the cell lysates were separated by 10% SDS-PAGE and transferred to a nitrocellulose membrane blocked with 5% skimmed milk and incubated with the primary antibodies (1:1,000 dilutions). The membranes were washed and the respective membranes were probed using antibodies for VEGF, Bcl-2, p53, BAX and GAPDH (as loading control) overnight at room temperature. The blots were washed and immunoreactive bands were incubated with a 1:2000 dilution of HRP (horseradish

peroxidase) conjugated secondary antibody for 2 h at room temperature. Binding signals were visualized with TMB (3, 3', 5, 5' Tetramethylbenzidine) substrate. Relative band intensities were determined with Image J software.

Sarcoma-180 solid tumor model

Sarcoma-180 ascites tumor cells (2×10^6 cells) were implanted subcutaneously into the left hind of the experimental mice. 10 days after inoculation, the test drug, PLL (20 and 40 mg/kg/b.w.) and standard drug 5-fluorouracil (5-FU, 20mg/kg/b.w.) were administered through i.p. injection for 21 consecutive days. The tumor volume was determined by direct measurement with verniercalipers every 2 days after the tumor implantation and the tumour inhibition was calculated (Ham et al., 2009; Maeda et al., 2009). On day 22, the animals were sacrificed by cervical dislocation and the tumors were removed for evaluation of various antitumor activities.

Tumor volume

The ratio of the developing tumors was measured using Verniercalipers at 2 day intervals for 21 days and the tumor volume was calculated using the formula:

$$V = \pi / 6 \times D_1 \times (D_2)^2$$

Where, D_1 is the longer diameter and D_2 is the shorter diameter.

Tumor weight

At the end of 21 days, all tumors (2 discs / animals) were punched out, weighed immediately, and the average weights were calculated. All tumors were excised and divided into two portions. One was used for SEM study and the other for histopathological and immunohistochemical analysis. The percentage inhibition was calculated by the formula:

$$\% \text{Inhibition} = 1 - B/A \times 100.$$

Where, A is the average weight of the control group and B is the average tumor weight of the treated group.

Estimation of blood haematological parameters

After 21 days of the treatment, animals were sacrificed by cervical dislocation and blood samples were collected from the heart using heparinized syringes for all types of haematological parameters.

Percentage increase in lifespan (%ILS)

After sacrifice, 3 mice from each group were observed for mean survival time (MST). The effect of PLL on percentage increase in lifespan (%ILS) was calculated on the basis of mortality of the experimental mice.

$$\text{Mean Survival time} = \frac{\sum \text{survival time (days) of each mouse in a group}}{\text{Total number of mice}}$$

$$\% \text{ ILS} = \frac{\text{MST of treated group}}{\text{MST of control group}} \times 100$$

(Sunil, Dhanya, et al., 2013)

H&E staining of sarcoma-180 tumor section

On day 21, the mice were sacrificed, tumors that developed at the site of injection were excised and fixed

in 10% formaldehyde and embedded in paraffin and 5 μ m sections were stained with hematoxylin and eosin (H&E). The slides were examined for histopathological changes such as a necrosis, mitotic figures and inflammatory reactions using light microscopy. 3 animals per group were used for histological and immunohistochemical analysis.

Scanning electron microscopy (SEM) study

After isolating a fine tissue section of test drug (PLL) treated and untreated solid tumor, they were prepared for scanning electron microscopy (SEM) study. On completion of ultrasonic cleaning, the tissue sections were fixed in 2.5% glutaraldehyde for 1 h at 4°C, washed in PBS, stained in 1% osmium tetroxide for 1 h at 4°C, followed by washing in PBS, dehydrated using ethanol, displaced in isoamyl acetate, dried at the critical point, gold coated and studied using scanning electron microscope (Quanta 200; Philips/FEI, Hillsboro, OR)(Xie QJ et al., 2014).

Immunohistochemistry study

Immunohistochemical analysis of Bcl-2, p53 and CD31 proteins in ~5 μ m thick tumor section was carried out. Briefly, the sections were hydrated in 1 X PBS for 5min. Antigen retrieval was performed by incubating the sections in 10 mM sodium citrate buffer (pH 6.0) at 80°C for 10 min. The sections were cooled to room temperature for 20 min. Following a 5-min wash with 1 X PBS, the endogenous peroxides were blocked by 1% hydrogen peroxide in PBS for 5min. The sections were washed as before and blocked for 1h. in PBS containing 1.5% normal serum. The slides were incubated overnight with primary antibodies respectively against CD31, Bcl-2 and p53 at 4°C in a humidified chamber. After washing with PBS, the sections were incubated with horseradish peroxides (HRP) – conjugated secondary antibodies at 1:100 dilutions for 30 min. at 37°C. The immune reactions were visualized by immersing the slides in 3, 3'-diaminobenzidine tetrahydrochloride reagent. The sections were counter stained with hematoxylin. Negative control sections were processed simultaneously with the omission of the primary antibodies. All sections were dehydrated, mounted viewed under light microscope (Eclipse TS100, Nikon, Japan) and photographed (10X).

Statistical analysis

All the results values were expressed as mean \pm standard error of mean (SEM). Experimental results were analyzed by student's t-test and One-way analysis of variance (ANOVA), followed by Kruskal Wallis Test using SPSS statistical software of 20.0 version. $P < 0.05$ was considered to be statistically significant when compared with control.

Results

In-vitro study

Cell viability assay

To characterize the activity in biological systems, the anti-proliferative activities of the compound PLL were determined in human erythroleukemic cell K562, human lung cancer cell A549, human macrophage cell U937 and

murine melanoma cell B16F10 using MTT assay. PLL growth inhibition against human cancer cells, with IC_{50} values of $3.36 \pm 0.16 \mu M$, $8.23 \pm 0.41 \mu M$, $3.53 \pm 0.17 \mu M$ and $6.04 \pm 0.3 \mu M$ for K562, A549, U937, and B16F10 cells respectively (Figure 2). These results indicate that the PLL contribute towards the anti-proliferative activities of the PLL in cancer cells. Among the cancers cells (K562, A549, U937, and B16F10), PLL is the most potent in K562 cells.

In-vivo study

PLL inhibits tumor growth of EAC cells

(Table 1) showed that, PLL at 20 and 40 mg/kg b.w (group II and III) significantly reduced the ascite fluid volume, packed cell volume and viable tumor cell count, whereas, increased non-viable tumor cell count in a dose dependent manner as compared to the control group. Furthermore, the median survival time (MST), also, exhibited a similar result, showing MST of 30.86 ± 0.43 days, compared to the control of 20.14 ± 0.02 days, respectively.

Effect of PLL on haematological parameters

Treatment with PLL at doses of 20 and 40 mg/kg b.w significantly increased the hemoglobin counts towards the normal levels. The RBC count was restored back to normal range on treatment with PLL (40 mg/kg b.w). PLL at an optimal dose of 40 mg/kg b.w could bring down the WBC level. In the differential count, lymphocytes and monocytes were found to be in a decreased level and the neutrophils were increased in the EAC control group when compared with the healthy group. PLL treatment at different doses as above significantly changes the relevant parameters approximately, to the normal values (Table 2).

Effect of PLL on biochemical parameters

(Table 3) demonstrates the biochemical parameters SGOT, SGPT, SALP and bilirubin significantly decreased at a dose dependent manner (20 and 40 mg/kg b.w.) as compared to EAC control group. Results show total protein contents also increased dose dependently.

Histopathology of liver tissue

H&E stained sections of liver slices of healthy mice, shown in panel A of (Figure 3), exhibiting the presence of all the normal features, including circular hepatic portal vein and branch of hepatic artery, as marked by arrows. The hepatocytes show prominent nuclei (Figure. 3, panel A, subpanel (i), marked by arrow) and the tissue section comprises hepatic sinusoids as usual. On the contrary, for the EAC control mice (Figure 3, panel B), none of the regular features as above mentioned could be found, rather, it reveals extensive hepatocellular lesions, as shown in subpanel (ii), as pyknotic nuclei (marked by arrow), exhibiting necrotic hepatocytes. On treatment using 5-FU, the cellular features were found to be close to normal, as shown in (panel C of Figure 3), although some irregularities, e.g., deformity in the hepatic artery and irregular bile duct could also be found. On treatment using the test drug, PLL at a dosage of 20 mg/kg b.w, very less amount of phenotypical alteration and altered hepatocyte population were found (Figure 3, panel D),

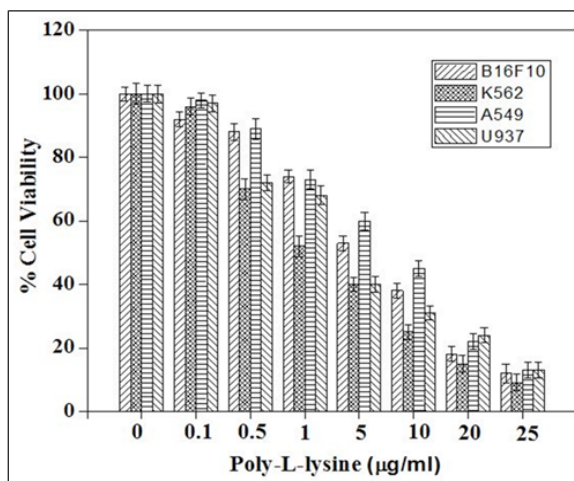


Figure 2. Analysis of Cytotoxic Potential of PLL. Data are expressed as mean \pm standard error of mean, $n=3$. K562, Human erythroleukemia cell; A549, human lung cancer cell; U937, human macrophage cell; B16F10, murine melanoma cell

marked by the presence of healthy hepatocytes (marked by box) although a mild dilation of the central vein could be observed. On escalation of the dose to 40 mg/kg b.w, (Figure 3, panel E) the cellular and overall features were close to normal as has been shown in panel A, marked by the presence of healthy hepatocytes (box), regular central vein, branch of bile duct and hepatic artery (marked by arrows) exhibiting the superiority of the same.

Changes in the morphology of EAC cells

The inhibitory effect of PLL on EAC cells of the mice model as mentioned above was observed both by

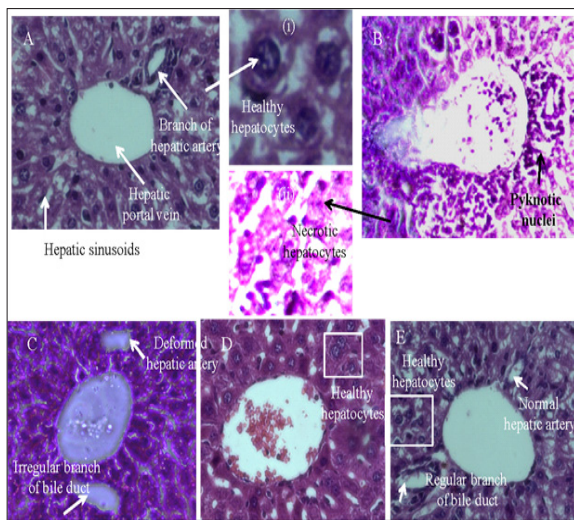


Figure 3. H and E Section of Liver from Mice Showing Hepatocellular Profile of (20 mg/kg b.w) Group (Figure 3, panel D), showed cellular infiltration, congestion and mild central vein dilation. PLL (40 mg/kg b.w) treated group (Figure 3, panel E) showed moderate/less neoplastic focal lesions, almost normal hepatocellular architecture (Figure 3, panel A, subpanel (i), marked by arrow) has been observed suggesting less hepatotoxicity. Whereas in EAC control mice (Figure 3, panel B), reveals extensive hepatocellular lesions, as shown in subpanel (ii), as pyknotic nuclei (marked by arrow), exhibiting necrotic hepatocytes.

Table 1. Effect at PLL on Ascite Fluid Volume, Packed Cell Volume, Body Weight, Mean Survival Time (MST), Percentage Increased Life Span (% ILS), Viable and non-Viable Tumor Cell Count in EAC Bearing Mice

	Poly L-lysine 20 mg/kg b.w	Poly L-lysine 40 mg/kg b.w	Std drug 20 mg/kg b.w	EAC Control(2 x 10 ⁶ cells/ mouse)
Ascite fluid volume (ml.)	6.63 ± 0.18*	4.6 ± 0.04*	5.18 ± 0.29*	11.55 ± 0.05*
Packed Cell volume (ml.)	2.73 ± 0.03*	1.45 ± 0.03*	1.34 ± 0.01*	3.97 ± 0.04*
Body Weight (gm.)	23.64 ± 0.24*	17.08 ± 0.08*	20.4 ± 0.25*	30.6 ± 0.27*
MST (days)	30.86 ± 0.43*	40.55 ± 0.04*	53.05 ± 0.04*	20.14 ± 0.02*
% ILS	56.25 ± 0.04	88.35 ± 0.05	112.35 ± 0.03	0 ± 0
Viable cell (x 10 ⁶ cells/ml)	3.05 ± 0.03*	1.23 ± 0.02*	3.32 ± 0.03*	10.07 ± 0.04*
Nonviable cell (10 ⁶ cells/ml)	3.98 ± 0.17*	3.79 ± 0.14*	3.99 ± 0.12*	0.67 ± 0.06*

Each point represent the mean ±SEM. (n=6 mice per group); *p<0.05 statistically significant when compared with EAC control group.

Haematoxylin & Eosin (H&E) and Papanicolaou (Pap) staining, as shown in (Figure 4). Of this, (Figure 4 A to D) corresponds to H&E staining that demonstrates blebbing of plasma membrane (marked by arrow), shown in [Figure 4D, panel (i)], whereas, the formation of apoptotic bodies could also be observed in [Figure 4D, panel (ii)]. In general, the control (EAC cells) cells have good circular morphology, intact plasma membrane and nucleus (Figure 4A), whereas, in case of the standard (5-FU), the apoptotic bodies and the nuclear condensation is evident (marked by arrow, Fig: 4B). In the PLL drug treated group for the dose 20 mg/kg b.w, chromatin condensation, blebbing of plasma membrane, irregularity

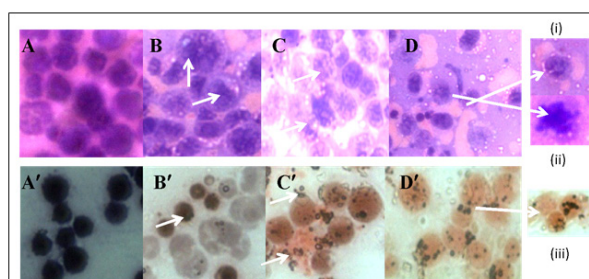


Figure 4. Change in Morphology of the EAC Cells by H and E Stain (A) control (B) standard (5-FU) (C) PLL, 20 mg/kg b.w (D) PLL, 40 mg/kg b.w and by Papanicolaou staining (A') control (B') standard (5-FU) (C') PLL, 20 mg/kg b.w (D') PLL, 40 mg/kg b.w. Panel (i) and (ii) of Figure 4 (D) show cellular blebbing and apoptotic body respectively and panel (iii) of Figure 4(D)' show nuclear fragmentation.

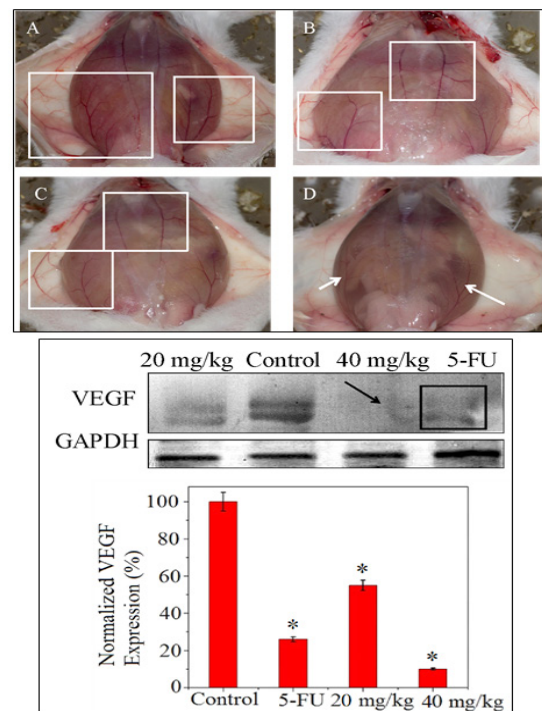


Figure 5. Angio Inhibitory Activity Profile of PLL Drug Shown in Part A, subpanel (A) EAC control (B) Standard drug, 5-FU (C) PLL, 20 mg/kg b.w (D) PLL, 40 mg/kg b.w. Part B of the figure shows the protein (VEGF) expression corresponding to angiogenesis and the densitometric analysis of the VEGF protein by western blot method.

in cell morphology, is observed in (Figure 4C), (marked by arrow). As the dose of PLL is escalated to twice the former, i.e., 40 mg/kg b.w, exhibited in (Figure 4D), both the phenomenon of cellular blebbing [Figure 4D, panel (i)] followed by cell shrinkage, cytoplasmic irregularity and formation of apoptotic body [Figure 4D, panel (ii)]. On staining of the cells using Pap dye, a number of features corresponding to cellular apoptosis is observed in both the cases of test groups treated with PLL (doses, 20 and 40 mg/kg b.w) characterized by chromatin condensation, heterochromatinization (Figure 4B', marked by arrow), nuclear fragmentation irregular shape, shrinkage of cell [Figure 4 C', D', panel (iii), all marked by arrow], confirming apoptosis in the treated EAC cells.

PLL inhibits peritoneal angiogenesis on in-vivo Ehrlich ascites tumor model

In a fully grown ascites tumor *in-vivo* (EAC control), there is an extensive skin peritoneal angiogenesis and neovascularization, as shown in part A of (Figure 5), subpanel A, marked by rectangular boxes, on treatment of the same using 5-FU (20 mg/kg b.w) the above features were observed to have a reducing trend, as seen in subpanel B (marked in rectangular boxes). On administration of the test drug 20 mg/kg b.w, a similar trend as in the case of the standard (5-FU), could be obtained (marked in rectangular boxes), whereas on escalating the dose of PLL to two times the previous (40 mg/kg b.w), an extensive suppression of the phenomenon of angiogenesis and neovascularization was observed (marked by arrow), demonstrating a better

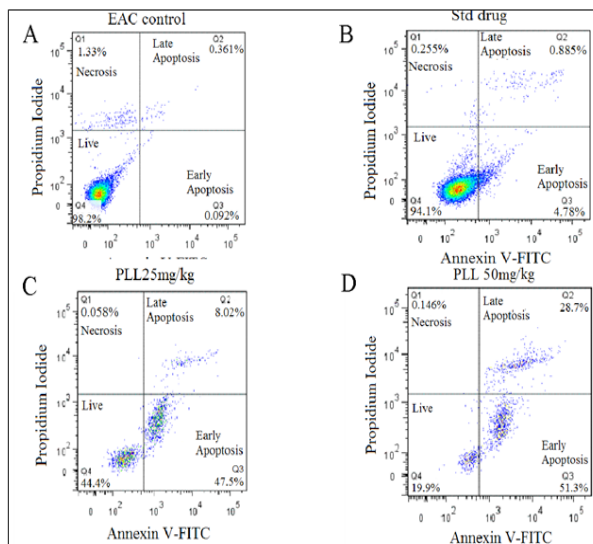


Figure 6. Apoptosis of EAC Cell Using PLL Treatment. Dot plot suggested that more number of apoptosis occurred at the higher dose of PLL (40 mg/kg b.w) (upper left, dead cells; lower left, live cells; upper right, left apoptotic cells; lower right, early apoptotic cells).

therapeutic efficacy of the test drug at the specific dose (40 mg/kg b.w), compared to the standard drug at a recommended dose as above, in EAC control mice.

To corroborate the observation as above corresponding to the EAC control, standard and the test drugs, western

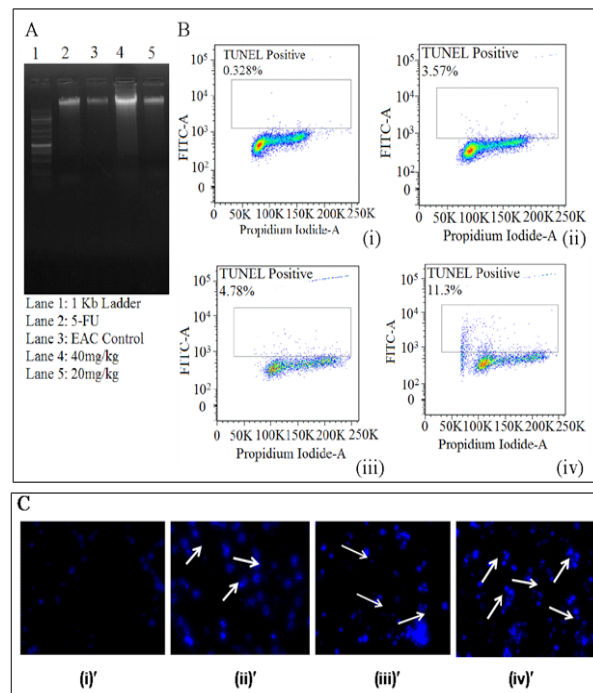


Figure 7. (A) DNA Fragmentation assay showing the corresponding descriptions in the Lanes, Exhibiting the Maximum Effect Corresponding to the PLL Dose 40 mg/kg b.w (B) TUNEL assay exhibiting apoptotic cell death for (i) control EAC cells (ii) standard drug (5-FU) (iii) PLL dose 20 mg/kg b.w (iv) PLL dose 40 mg/kg b.w, exhibiting the maximum apoptosis corresponding to the PLL dose 40 mg/kg b.w. (C) DAPI staining showing (i)' control EAC cells (ii)' standard drug (5-FU) (iii)' PLL dose 20 mg/kg b.w (iv)' PLL dose 40 mg/kg b.w, exhibiting the maximum apoptosis corresponding to the PLL dose 40 mg/kg b.w.

Table 2. Effect of PLL on Haematological Parameters in EAC Bearing Mice

	Poly L-lysine 20 mg/kg b.w	Poly L-lysine 40 mg/kg b.w	Std drug 20 mg/kg.b.w	EAC Control (2 x 10 ⁶ cells/ mouse)	Normal Mice
Hemoglobin (gm %)	8.37 ± 0.01*	8.77 ± 0.02*	8.88 ± 0.02*	6.44 ± 0.19*	12.4 ± 0.14
Erythrocyte (RBC) (cells x 10 ⁶ /mm ³)	6.94 ± 0.02*	7.41 ± 0.02*	6.7 ± 0.02*	4.39 ± 0.02*	9.59 ± 0.03
Leucocytes (WBC) (cells x 10 ⁶ /mm ³)	12.35 ± 0.03*	9.73 ± 0.02*	8.22 ± 0.02*	18.14 ± 0.03*	13.4 ± 0.03
Neutrophil (%)	31.17 ± 21.91*	30.13 ± 0.03*	41.22 ± 0.02*	72.14 ± 0.06*	30.09 ± 0.06
Lymphocyte (%)	44.76 ± 0.11*	53.83 ± 0.02*	61.05 ± 0.04*	34.06 ± 0.05*	68.34 ± 0.25
Monocyte (%)	1.72 ± 0.02*	2.31 ± 0.03*	1.78 ± 0.02*	1.19 ± 0.03*	2.14 ± 0.03

blot analysis of the protein expression corresponding to the phenomenon of angiogenesis and neovascularization was undertaken, which has been illustrated in (Figure 5 part B), showing the minimum level (15-18%) of the protein (VEGF) expression at a dose of 40 mg/kg b.w of PLL test drug. This observation is at par with the corresponding band intensity (marked by arrow) which does not exhibit VEGF expression, compared to the faint expression levels corresponding to the standard drug (marked by rectangular box) and PLL at a dose of 20 mg/kg b.w.

Study of apoptosis in in-vivo EAC cells by TUNEL assay, DNA fragmentation and DAPI staining

Here, EAC cells treated with various doses of PLL showed apoptosis in a dose dependant manner as evidenced by the internucleosomal DNA fragmentation,

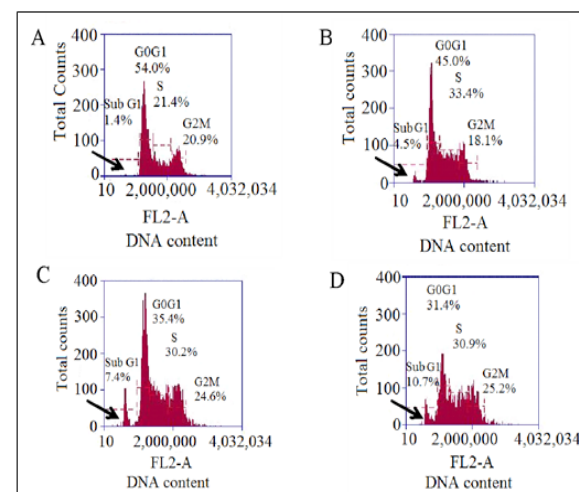


Figure 8. Cell Cycle Analysis by Flow Cytometry Showing A.) EAC control B.) Standard (5-FU) C.) 20 mg/kg b.w D.) 40 mg/kg b.w, the variation in the DNA content corresponding to the sub G1 phase (apoptotic phase), marked by arrow.

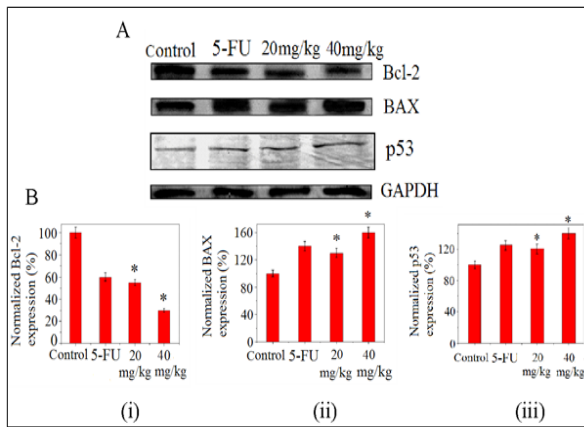


Figure 9. (A)Western Blot assay for the changes of Bcl-2, Bax and p53 Proteins in EAC Tumor Cell after Treatment of PLL.(B) Densitometric analysis showing (i) down-regulation of Bcl-2 expression whereas (ii) and (iii) shows up-regulation of Bax, p53 expressions. Each value represents the mean (\pm SD) of three independent experiments, each performed in triplicates (* p <0.05).

shown in (Figure 7A). As seen, the maximum smear is obtained at a dose of 40 mg/kg b.w, indicating a major fragmentation, characterized by the activation of endogenous endonucleases with subsequent cleavage of chromatin DNA into internucleosomal fragments, although for the cases using standard drug, 5FU and test drug PLL at a dose of 20 mg/kg b.w shows the same at a lesser extent. Such observation demonstrates apoptosis of EAC cells in the present case, induced by the particular dosage of PLL, as above, encompassing characterized by the activation of endogenous endonucleases with subsequent cleavage of chromatin DNA into internucleosomal fragments.

The above observation in turn have been corroborated by TUNEL assay, shown in (Figure 7B), revealing an exponential escalation of the percentage of cells that has undergone a programmed cell death, in a dose dependent manner. Such observation was further confirmed using DAPI staining (Figure 7C) that can be directly correlated to the phenomenon of chromatin condensation, which occurred at a maximum level in case of the test dose of 40 mg/kg b.w of PLL, compared to the rest, as shown by arrow.

Cell cycle analysis by flow cytometry

The typical changes of cell cycle profile induced by

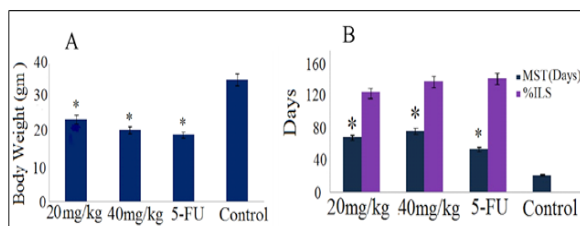


Figure 10. Effect of PLL Treatment on (A) body weight and (B) mean survival time (MST), percentage of increase life span (%ILS) of sarcoma-180 bearing mice, standard drug (5-FU) and control.* p <0.05 statistically significant when compared with sarcoma-180 control group.

Table 3. Effect of PLL on Serum Biochemical in EAC Bearing Mice

	Poly L-lysine 20 mg/kg b.w	Poly L-lysine 40 mg/kg b.w	Std drug 20 mg/kg.b.w	EAC Control (2 x 10 ⁶ cells/mouse)	Normal Mice
Bilirubin Total & Direct : (mg/dl)	0.31 \pm 0.01*	0.26 \pm 0.02*	0.26 \pm 0.01*	0.37 \pm 0.01*	0.42 \pm 0.02
Conjugated (mg/dl)	0.16 \pm 0.04*	0.12 \pm 0.03*	0.13 \pm 0.04*	0.14 \pm 0.04*	0.21 \pm 0.02
Unconjugated (mg/dl)	0.15 \pm 0.04*	0.14 \pm 0.04*	0.13 \pm 0.03*	0.23 \pm 0.04*	0.21 \pm 0.01
Serum Protein (Total) (mg/dl)	6.28 \pm 0.08*	6.62 \pm 0.08*	6.74 \pm 0.11*	2.34 \pm 0.11*	6.82 \pm 0.08
Albumin (mg/dl)	2.22 \pm 0.77*	2.92 \pm 0.29*	2.86 \pm 0.37*	1.2 \pm 0.07*	2.92 \pm 0.44
Globulin (mg/dl)	4.06 \pm 0.7*	3.7 \pm 0.37*	3.88 \pm 0.35*	1.14 \pm 0.05*	3.9 \pm 0.37
AST(SGOT) (IU/L)	55.49 \pm 0.07*	36.1 \pm 0.03*	31.12 \pm 0.02*	78.09 \pm 0.05*	38.17 \pm 0.03
ALT (SGPT) (IU/L)	47.15 \pm 0.02*	32.33 \pm 0.04*	30.06 \pm 0.04*	66.34 \pm 0.03*	28.35 \pm 0.03
Serum Alkaline Phosphates (IU/L)	98.23 \pm 0.03*	79.12 \pm 0.02*	72.93 \pm 0.03*	123.26 \pm 0.03*	77.25 \pm 0.01
Creatinine (mg/dl)	0.76 \pm 0.01*	0.8 \pm 0.02*	0.56 \pm 0.01*	0.62 \pm 0.02*	0.82 \pm 0.02

PLL (test drug, dose as above) is shown in (Figure 8), obtained by flow cytometry analysis, that showed a dose dependent increase in the sub-G1 population (hypodiploid DNA content) of cells, which is a hallmark of apoptosis. In case of EAC peritoneal tumor model, on day 14, it was observed the content of the hypodiploid DNA was

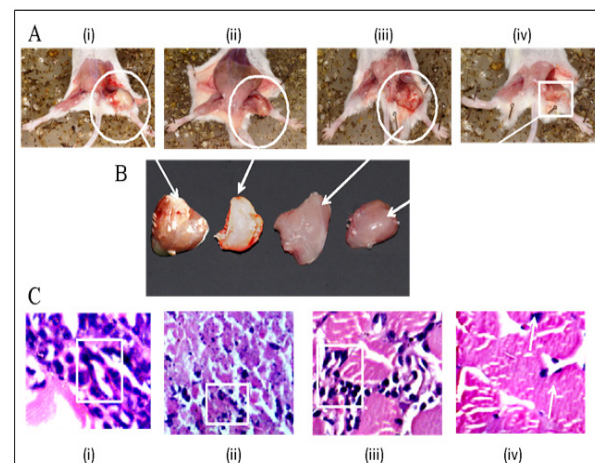


Figure 11. Effect of PLL Treatment on Solid Sarcoma-180 Tumor: panel (A), subpanel (i) sarcoma-180 control (ii) 5-FU drug treated (iii) 20 mg/kg b.w PLL treated and (iv) 40 mg/kg b.w PLL treated. Panel (B) shows the dissected tumor tissues in the same order as in (A) above, marked by arrows and circles. Panel (C) H & E stained histological section of the solid tumour in the order as in panel (A) above, (i) control (ii) 5-FU (iii) 20 mg/kg b.w (iv) 40 mg/kg b.w, the cellular features are marked by boxes.

Table 4. Effect of PLL on Tumor Weight, Percentage of Tumor Volume, Body Weight, Mean Survival Time (MST) and Percentage Increase Life Span (%ILS) on Sarcoma-180 Solid Tumor Bearing Mouse

	Poly L-lysine 20 mg/kg b.w	Poly L-lysine 40 mg/kg b.w	Std drug 20 mg/kg. b.w	Sarcoma-180 Control (2 x 10 ⁶ cells/ mouse)
Tumor weight (gm.)	8.1 ± 0.04*	4.32 ± 0.05*	3.4 ± 0.04*	17.23 ± 0.13*
% Tumor volume	82.39 ± 0.07*	82.75 ± 0.06*	75.68 ± 0.07*	0 ± 0
Body weight(gm.)	23.64 ± 0.54*	20.63 ± 0.71*	19.18 ± 0.13*	35.02 ± 0.56*
MST(days)	72.16 ± 0.15*	78.38 ± 0.28*	55.5 ± 0.34*	22.5 ± 0.27*
% ILS	131.09 ± 0.08	142.84 ± 0.82	146.68 ± 0.27	0 ± 0

increased in the sub-G1 population for group II mice, at 20 mg/kg b.w dose (from 1.4% to 7.4 %) which in turn was enhanced in dose dependent manner (40 mg/kg b.w) (to 10.7%) confirming the DNA damage as above mentioned. When compared with the standard drug, 5-FU (4.5%), the result obtained was < the PLL test drug at a dosage of 20 mg/kg b.w.

Assessment of protein level expression of PLL induced apoptosis

It is well known that, when cells become committed to apoptosis it partly depends upon the balance between tumor suppressor protein p53, anti-apoptotic factors, including Bcl-2 and pro-apoptotic factors such as Bax (Toshiyuki et al., 1995; Oltval et al., 1993; de – Aguilar et al., 2000). Our result show, the level of p53 and Bax protein expressions increase significantly in test drug treated tumor bearing mice in comparison to EAC control

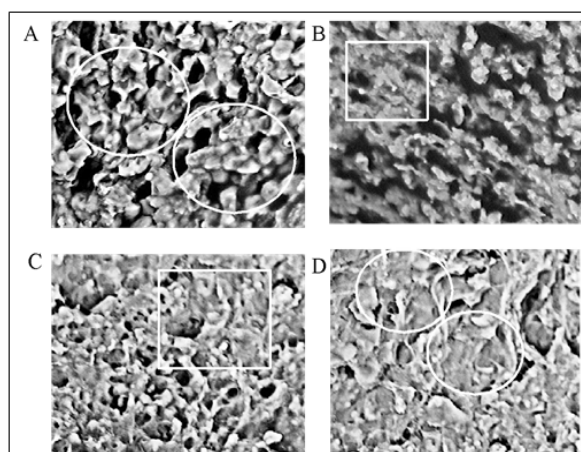


Figure 12. PLL Induced Cell Apoptosis Arrayed by Scanning Electron Microscope (SEM). In control group (panel A) cells numerous long microvilli can be seen on the rough surface, whereas sarcoma-180 cells treated with PLL (20 mg/kg b.w and 40 mg/kg b.w) (panel C, D) and on treatment with standard drug 5-FU decreased number and length of microvilli, smoothening of cell surface and apoptotic bodies formed (magnification: 1000X).

Table 5. Effect of PLL on Haematological Parameters in Sarcoma-180 Solid Tumor Bearing Mice

	Sarcoma-180 Control (2 x 10 ⁶ cells/ mouse)	Poly L-lysine 20 mg/ kg b.w	Poly L-lysine 40 mg/kg b.w	Std. drug 20 mg/kg. b.w	Normal mice
Hemoglobin (gm %)	10.2± 0.01*	7.3± 0.05*	8.9± 0.08*	8.6± 0.08*	13.9± 0.12*
Erythrocytic (RBC) (million/mm ³)	3.79± 0.04*	4.48± 0.04*	5.8± 0.03*	5.7± 0.03*	6.90± 0.02*
Leucocytic (WBC) (10 ³ cells/mm ³)	16.86± 0.02*	11.18± 0.05*	5.11± 0.05*	4.25± 0.05*	4.85± 0.09 *
Neutrophil	68.4± 0.05*	42.35± 0.03*	26.4± 0.02*	30.1± 0.02*	17.5± 0.03*
Lymphocyte (%)	35.1± 0.11*	45.0± 0.04*	63.0± 0.09*	65.0± 0.09*	68.2± 0.25*
Monocyte (%)	1.6± 0.04*	1.7± 0.03*	1.7± 0.03*	1.8± 0.03*	2.3± 0.02*

Each point represent the mean ±SEM; (n, 6 mice per group); *p<0.05 statistically significant when compared with EAC control group.

mice (Figure 9, panel B, subpanel (ii), (iii)). The level of Bcl-2 though initially high in control EAC bearing mice but decreases upon exposure to PLL and thereby resulting in an increase in Bcl-2/ Bax ratio (Figure 9B). It is known that, p53 is capable of down-regulating the antiapoptotic protein Bcl-2 and up-regulating pro-apoptotic protein, Bax, thus, confirming the results in these experiments.

PLL inhibits tumor growth within sarcoma-180 solid tumor

(Table 4) shows that, PLL at 20 mg/kg b.w and 40 mg/kg b.w reduced the solid tumor volume and weight significantly at the end of 21 days, compared to the control. In PLL treated groups, the body weight was also reduced significantly on all the monitored days (Figure 10A).

The Hb counts were lower in all the PLL treatment groups in compared to sarcoma-180 control group. The RBC count was restored back to normal range on treatment

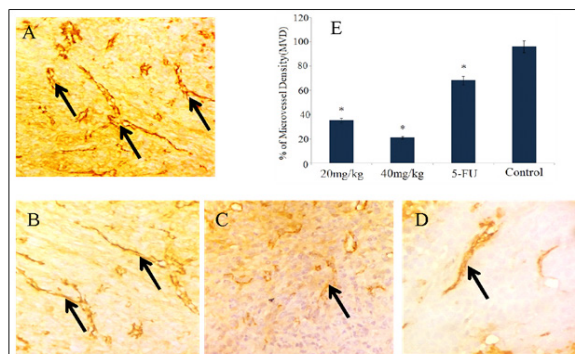
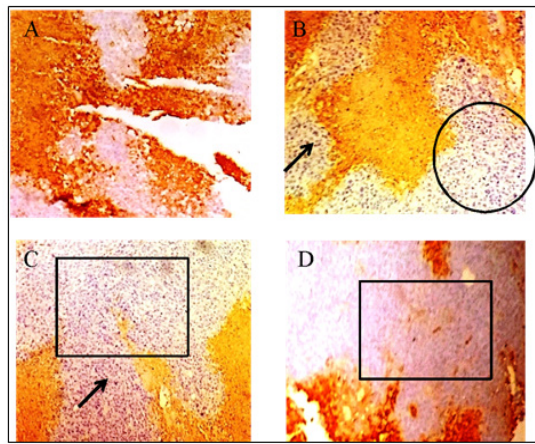
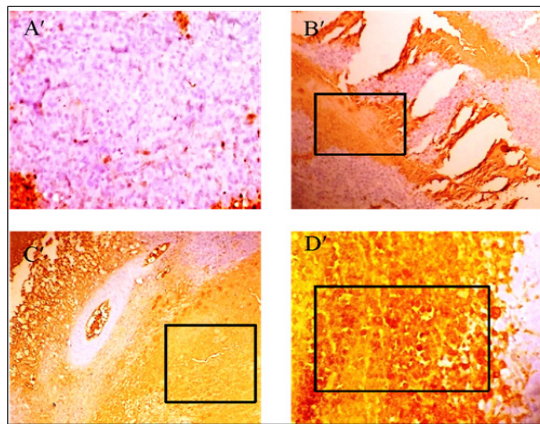


Figure 13. Immunostaining and Optical Density of CD31 Expression in Swiss Albino Mice. (Magnification: 400X). (A) Control (sarcoma-180) (B) 5-FU (C) 20 mg/kg b.w (D) 40 mg/kg b.w, exhibiting the reduction of neovascularization (arrow marked) in the order as shown. Each bar represents the mean ±SD (n=3 tumors). *p<0.05 as compared to control group.



Part A



Part B

Figure 14. Immunohistochemistry of Part A, Panel (A) sarcoma-180 control (B) 5-FU (C) 20mg/kg and (D) 40mg/kg, showing Bcl-2 (anti-apoptotic protein) expression, in a reducing manner in the above order, marked by box, circle and arrow. Part B exhibits p53 (tumour suppressor protein) expression in an increasing manner in the order panel (A') sarcoma-180 control (B') 5-FU (C') 20 mg/kg b.w and (D') 40 mg/kg b.w. as above, shown in boxes. Started from day 10 of tumor implantation and continued for 21 days (Magnification: 100 X).

with PLL (40 mg/kg b.w). PLL at an optimal dose of 40 mg/kg b.w could bring down the WBC level compare to Sarcoma-180 control group. The neutrophils were decreased and lymphocytes were increased significantly in all the treated groups compared with sarcoma-180 control group. PLL treatment at different doses as stated above showed significant changes with approximately to the normal values (Table 5).

PLL enhances the survival of sarcoma-180 bearing mice

The survival of sarcoma-180 bearing mice significantly increased as compared to sarcoma-180 bearing control group. The %ILS in PLL at 20 and 40 mg/kg was found to be in a dose dependent manner (Figure 10B).

Effect of PLL on histopathological changes of solid sarcoma-180 tumor

After fixation in formaldehyde, tumor parts were grossly examined for size or colour changes and hemorrhage (Figure 11, panel A and B, marked by

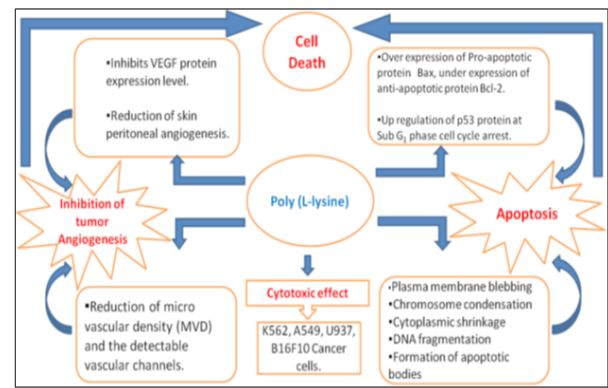


Figure 15. Schematic Diagram of Anti-Cancer Activity of PLL on In-Vitro and In-Vivo Cancer Cell Lines

arrow and circles). Histopathological analysis of the solid tumors from control mice showed sheets of large round and polygonal cells, with pleomorphic shapes, hyperchromatic nuclear and binucleation. Several degrees of cellular and nuclear pleomorphism were seen, marked by boxes in (Figure 11, panel C, subpanel (i) to (iv)). In the tumors extirpated from animals treated with test drug PLL in different doses (20 and 40 mg/kg b.w.) and in 5-FU, extents areas of coagulative necrosis showed less proliferation and muscle invasion were also observed (Figure 11, panel (C), subpanel (ii) to (iv)). Such finding was significantly improved in mice treated with PLL as evident by progressively increasing multiple apoptotic bodies, fibro skeletal muscle fiber and lymphoid aggregation show some malignant cell infiltration, as shown in Figure.11, panel C, subpanel (iii) and (iv).

Scanning electron microscopy analysis of solid sarcoma-180 tumor

SEM examination revealed that, in case of control group, cancer (sarcoma-180) cells were found with intact nuclear membrane with huge and circular nuclei, numerous long microvilli (Figure 12, panel A, marked in circles), while, on treatment with 5-FU, these cells were less in number (Figure 12, panel B, marked in box) and exhibit a shrunken morphology with nuclear membrane lumped, disrupted with decreased surface microvilli. Similar observation was obtained in case of the test drug (PLL) treated cases of the doses, 20 mg/kg b.w and 40 mg/kg b.w (Figure 12, panel C, marked in box and panel D, and marked in circles) in the order as mentioned, where nuclear membrane was disrupted, cells were shrunken, the nuclei were broken and the dense network of microvilli was decreased.

PLL induces apoptosis by triggering the expression of p53 and Bcl-2

We studied the expression of Bcl-2, anti-apoptotic protein and p53 a tumor suppressor protein in solid Sarcoma-180 tumor samples. Here we examined the regression in tumor growth by PLL, due to the induction of apoptosis that decreased the expression of Bcl-2, which is basically an anti-apoptotic protein (Figure 14 part A, panel A to D) demonstrated by the decrease in the yellow brown colour (due to horseradish peroxidase, HRP conjugated

secondary antibody) that denotes the protein. On the contrary, a progressive enhancement in the expression of p53 (Figure 14, part B, panel A' to D') protein (tumor suppressor protein), exhibited by brownish yellow color on cytoplasm and nuclei, compared to control, could be found, indicating an effective suppression of the tumor.

Discussion

Cancer cells are virtually immortal due to uncontrolled proliferation (Torre et al., 2015). A prospective anti-cancer drug is considered viable if it has the capacity to slow down the process of cell proliferation and trigger the signalling mechanism that initiates the process of apoptosis or cell death. The aim of this study was to determine whether PLL possesses anti-proliferative, apoptotic and suppression of angiogenic activity against an animal of EAC liquid and Sarcoma-180 solid tumor model.

It was demonstrated that PLL has *in vitro* cytotoxic effects on K562, A549, U937 and B16F10 cancer cells, which is noteworthy.

Apoptosis is a tightly regulated mechanism that is easily distinguished by its diverse alteration to the cells, including loss of plasma membrane asymmetry and attachment, cytoplasmic shrinkage, chromatin condensation, DNA fragmentation, nucleus and internucleosomal cleavage of DNA and the formation of apoptotic bodies (Hengartner et al., 2000). From our study we have observed morphological changes of cells, cytoplasmic shrinkage, membrane blebbing and formation of apoptotic bodies in both EAC and Sarcoma-180 cell lines. In this study DNA fragmentation was confirmed by agarose gel electrophoresis. The nuclear DNA of apoptotic cells shows a characteristic laddering pattern of oligonucleosomal fragments, which is regarded as the hallmark of apoptosis (Lin et al., 2011). Additionally, chromatin condensation and DNA damage were observed through DAPI staining of DNA in *in-vivo* EAC cell lines.

Apoptosis was further confirmed by annexin-V/FITC staining in EAC cell line. In apoptotic cells, the membrane phospholipids, phosphatidylserine (PS) is translocated from the inner to the outer leaflet of the plasma membrane, thereby exposing PS to the external cellular environment. Annexin-V has high affinity for PS and binds to the cells with exposed PS. FITC-conjugated Annexin-V can thus bind to apoptotic cells and can be identified by FACS (Seong et al., 2016). Since externalization of PS occurs in the earlier stages of apoptosis, Annexin-V/FITC staining can identify apoptosis at the early stage than assays by PI which is based on nuclear changes such as DNA fragmentation. Hence, FACS analysis indicates the early cells of apoptosis (Annexin-V-FITC positive cells) in test drug treated EAC tumor. This result is also contributing to the increase in cell death and consequent tumor growth inhibition. These observations provided clear evidence of the apoptotic potential of PLL in liquid EAC cancer cell.

The test results led us to investigate the modulation of p53 protein and cell cycle arrest of cancer cells after administration of the PLL. Up-regulation of p53 protein associated with cell cycle arrest at sub-G₁ stage clearly points out the actual cause of drug induced DNA damage

(Hynu et al., 2015). The over-expression of apoptotic protein Bax, the under-expression of anti-apoptotic protein Bcl-2 and the apoptotic assay studies with TUNEL assay clearly indicate that there were considerable changes in the balance of this protein ratio which triggered the beginning of the apoptotic process (Bhattacharyya et al., 2004). Post treatment of EAC cells with PLL a significant increase of Bax and decrease of Bcl-2 were observed. The altered ratio of pro-apoptotic and anti-apoptotic factors favoured the promotion of apoptosis. Therefore, PLL reduced the ability of Bcl-2 to bind to Bax and enhanced the translocation of Bax from cytosol to mitochondria, further increasing the susceptibility of the cells to apoptosis (ZuKe et al., 2005). The increase in both Bax/Bcl-2 protein ratio and p53 protein level in PLL treated cancer cells also proves the initiation of apoptosis, through the mitochondria-mediated intrinsic pathway.

The mechanism by the test drug induces antitumor effect also involved with anti-angiogenic activity. Tumor angiogenesis is the proliferation of a network of blood vessels that penetrates into cancerous growth. Increased neovasculature may allow not only an increase in tumor growth but also enhances hematogenous tumor immobilization. Thus inhibiting tumor angiogenesis may halt the tumor growth and decrease metastatic potential of tumors. Inhibition of fluid accumulation, tumor growth, and microvessel density by neutralization of VEGF has demonstrated the importance of VEGF in malignant ascites formation (Kim et al., 1993; Colombo et al., 2002). Our studies show that PLL inhibited tumor angiogenesis by inhibiting the secretion of VEGF dose dependently and prevented the formation of tumor directed capillaries resulting in reduced peritoneal angiogenesis in EAC bearing mice.

To study the activity of anti-angiogenic effect of PLL in *in-vivo* solid tumor model, we investigated the effect of CD31, one of the most commonly used endothelial cell markers that highlight tumor blood vessels and reflect degree of angiogenesis (Muller et al., 2002). Our result revealed that the activity of PLL produced a greater reduction in microvessel density (MVD). This indicates that the Sarcoma-180 tumor inhibition exerted by the PLL treatment was attributed to the angiogenesis suppression. The overall anticancer activity of PLL is demonstrated schematically (Figure 15).

The SEM study revealed that, PLL treatment significantly alters the morphological features of Sarcoma-180 cells. Further in PLL treated cells there was a marked reduction in the density and size of surface microvilli. Also cells appeared to be shrunk with the reduction of cellular volume and break up of nuclear membrane. These features also evaluate that, typical apoptosis appeared at various concentration of PLL treatment.

Treatment with PLL decreased tumor burden, inhibited tumor volume and viable cell count, reduced solid tumor size and weight and also increased the lifespan and survival time of EAC liquid and Sarcoma-180 solid tumor bearing mice. Prolongation of lifespan of animal has been well documented as criteria for judging the drug activity. Treatment with PLL normalized the Hb content, RBC

and WBC counts demonstrating protective action on the hematopoietic system.

Liver is an organ where detoxification process takes places, but many chemotherapeutic drugs accumulate their metabolic products in the liver, further aggravating toxicity. In this study, liver functions were investigated by biochemical estimations of AST, ALT and ALP levels and histopathological examination of liver tissue in mice given daily i.p injection of PLL at doses of 20 and 40 mg/kg b.w. of body weight. Treated animals with PLL demonstrated limited signs of overall toxicity in the parameters measured in this study. The treatment groups showed no alterations on total body weights in comparison with the control group.

Investigations in this study has shown the test compound, PLL, induced inhibition of EAC ascites and Sarcoma-180 solid tumor cell growth was due to the induction of apoptosis and suppression of tumor angiogenesis. Our *in-vivo* results also indicate that PLL could be effective as an anticancer agent, though additional studies are warranted.

In conclusion our study indicates PLL induced *in-vitro* cytotoxic effect in K562, A549, and U937 cancer cell lines and *in-vivo* tumor growth inhibition in EAC and Sarcoma-180 tumor models. These results clearly indicate that PLL significantly inhibits cell viability in a dose dependent manner in EAC & Sarcoma-180 cells. PLL also changes the morphology of cells and is able to induce Bcl-2 dependent apoptosis in both ascites EAC and solid Sarcoma-180 tumor via an intrinsic mitochondrial pathway. Our investigations demonstrate the expression of both p53 and Bax in the tumor cells increase significantly with the treatment of PLL, but reduce the level of Bcl-2, thereby resulting in increase of Bcl-2/Bax ratio, associated with sub-G₁ phase cell cycle arrest, substantiating apoptosis. PLL also exerts antiangiogenic effects by reduction of microvessel density, inhibition of angiogenic growth factor VEGF levels in early stages of tumor growth and through the down regulation of CD31 expression. Our results indicate PLL inhibits tumor cell proliferations via apoptotic pathway and tumor angiogenesis suppression. Although PLL has significant inhibitory effects on EAC and Sarcoma-180 cell lines, additional molecular mechanisms of PLL in *in-vitro* cancer cell lines and xenografts in nude mouse need to be investigated.

Conflict of interest

The authors declare that there are no conflicts of interests.

Acknowledgements

This work was supported by a grant of University of Grant Commission, New Delhi, India, sanctioned to Souvik Debnath through UGC-BSR Research Fellowship in Science for Meritorious Students fellowship scheme. Also given special thanks to Dr. Jyotirmayee Dash, Associate Professor, Department of Organic Chemistry, Indian Association for the Cultivation of Science, Kolkata, India for her very special guidance of experiments. We

also thank Dr. Sayed Mahmood Nadeem, Director and Chief Pathologist, N.G. Medicare, Kolkata, India and Dr. Avinaba Mukherjee, UGC Dskothari Post- Doctoral fellow, Jadavpur University, India for their kind assistance.

References

- Anghileri LJ, Heidbreder M, Mathes R (1976). Accumulation of ⁵⁷Co-poly-L-lysine by tumors: an effect of the tumor electrical charge. *J Nucl Biol Med*, **20**, 79.
- Arnold LJ, Dagan A, Simon SD, Kaplan NO (1978). Polymer-linked derivatives of nicotinamide analogs-elimination of toxic side-effects with an increase in anti-neoplastic activity. *Clin Cancer Res*, **19**, 114.
- Arnold LJ, Dagan A, Gutheil J, Kaplan NO (1979). Antineoplastic activity of poly (L-lysine) with some ascites tumor cells. *Proc Natl Acad Sci U S A*, **76**, 3246-50.
- Bhattacharyya A, Mandal D, Lahiry L, Sa G, Das T (2004). Black tea protects immunocytes from tumor-induced apoptosis by changing Bcl-2/Bax ratio. *Cancer Lett*, **209**, 147-54.
- Bichowsky-Slomnicki L, Berger A, Kurtz J, Katchalski E, (1956). The antibacterial action of some basic amino acid copolymers. *Arch Biochem Biophys*, **65**, 400-13.
- Britto AC, de Oliveira AC, Henriques RM, et al (2012). In vitro and in vivo antitumor effects of the essential oil from the leaves of *Guatteria friesiana*. *Planta Med*, **78**, 409-14.
- Bussolino F, Mantovani A, Persico G (1997). Molecular mechanisms of blood vessel formation. *Trends Biochem Sci*, **22**, 251-6.
- Carmeliet P, Jain RK (2000). Angiogenesis in cancer and other diseases. *Nature*, **407**, 249-57.
- Chen L, Watkins JF (1970). Evidence against the presence of H2 histocompatibility antigens in Ehrlich ascites tumour cells. *Nature*, **225**, 734-5.
- Colombo MP, Trinchieri G (2002). Interleukin-12 in anti-tumor immunity and immunotherapy. *Cytokine Growth Factor Rev*, **13**, 155-68.
- Cory S, Huang DC, Adams JM (2003). The Bcl-2 family: roles in cell survival and oncogenesis. *Oncogene*, **22**, 8590-607.
- Das T, Sa G, Sinha P, Ray PK (1999). Induction of cell proliferation and apoptosis: dependence on the dose of the inducer. *Biochem Biophys Res Commun*, **260**, 105-10.
- de Aguilar JLG, Gordon JW, René F, et al (2000). Alteration of the Bcl-x/Bax ratio in a transgenic mouse model of amyotrophic lateral sclerosis: evidence for the implication of the p53 signaling pathway. *Neurobiol Dis*, **7**, 406-15.
- Donati G, Montanaro L, Derenzini M (2012). Ribosome biogenesis and control of cell proliferation: p53 is not alone. *Cancer Res*, **72**, 1602-7.
- Ferrara N, Gerber HP, LeCouter J (2003). The biology of VEGF and its receptors. *Nat Med*, **9**, 669-76.
- Folkman J (1971). Tumor angiogenesis: therapeutic implications. *N Engl J Med*, **285**, 1182-6.
- Gayatri S, Reddy CUM, Chitra K, Parthasarathy V (2015). Assessment of in vitro cytotoxicity and in vivo antitumor activity of *Sphaeranthus amaranthoides* burm. f. *Pharmacogn Res*, **7**, 198.
- Green M, Stahmann MA (1953). Inhibition of Mumps virus multiplication by a synthetic polypeptide. *Proc Soc Exp Biol Med*, **83**, 852-8.
- Guo L, Lv G, Qiu L, et al (2016). Insights into anticancer activity and mechanism of action of a ruthenium (II) complex in human esophageal squamous carcinoma EC109 cells. *Eur J Pharmacol*, **786**, 60-71.
- Ham YA, Choi HJ, Kim SH, Chung MJ, Ham SS (2009). Antimutagenic and antitumor effects of *Adenophora triphylla* extracts. *J Korean Soc Food Sci Nutr*, **38**, 25-31.
- Hengartner MO (2000). The biochemistry of apoptosis. *Nature, Asian Pacific Journal of Cancer Prevention, Vol 18* **2267**

- 407, 770.
- Hyun SY, Jang YJ (2015). p53 activates G1 checkpoint following DNA damage by doxorubicin during transient mitotic arrest. *Oncotarget*, **6**, 4804.
- Kim KJ, Li B, Winer J, et al (1993). Inhibition of vascular endothelial growth factor-induced angiogenesis suppresses tumour growth in vivo. *Nature*, **362**, 841.
- Lee YL, Kim HJ, Lee MS, et al (2003). Oral administration of *Agaricus blazei* (H1 strain) inhibited tumor growth in a sarcoma 180 inoculation model. *Exp Anim*, **52**, 371-5.
- Lien HM, Lin HW, Wang YJ, et al (2011). Inhibition of anchorage-independent proliferation and G0/G1 cell-cycle regulation in human colorectal carcinoma cells by 4, 7-dimethoxy-5-methyl-1, 3-benzodioxole isolated from the fruiting body of *Antrodia camphorate*. *Evid Based Complement Alternat Med*, **2011**.
- Lowe SW, Lin AW (2000). Apoptosis in cancer. *Carcinogenesis*, **21**, 485-95.
- Maeda N, Kokai Y, Ohtani S, et al (2009). Inhibitory effects of preventive and curative orally administered spinach glycolipid fraction on the tumor growth of sarcoma and colon in mouse graft models. *Food Chem*, **112**, 205-10.
- McMahon G (2000). VEGF receptor signaling in tumor angiogenesis. *Oncologist*, **5**, 3-10.
- Mizuno T, Zhuang C, Abe K, et al (1999). Antitumor and hypoglycemic activities of polysaccharides from the sclerotia and mycelia of *Inonotus obliquus* (Pers.: Fr.) Pil. (Aphyllphoromycetidae). *Int J Med Mushrooms*, **1**.
- Mosmann T (1983). Rapid colorimetric assay for cellular growth and survival: application to proliferation and cytotoxicity assays. *J Immunol Methods*, **65**, 55-63.
- Müller AM, Hermanns MI, Skrzynski C, et al (2002). Expression of the endothelial markers PECAM-1, vWf, and CD34 in vivo and in vitro. *Exp Mol Pathol*, **72**, 221-9.
- Oltval ZN, Milliman CL, Korsmeyer SJ (1993). Bcl-2 heterodimerizes in vivo with a conserved homolog, Bax, that accelerates programmed cell death. *Cell*, **74**, 609-19.
- Ozaslan M, Karagoz ID, Kilic IH, Guldur ME (2011). Ehrlich ascites carcinoma. *Afr J Biotechnol*, **10**, 2375-8.
- Patt HM, Straube RL (1956). Measurement and nature of ascites tumor growth. *Ann NY Acad Sci*, **63**, 728-37.
- Reed JC (2000). Mechanisms of apoptosis. *Am J Pathol*, **157**, 1415-30.
- Samudrala PK, Augustine BB, Kasala ER, et al (2015). Evaluation of antitumor activity and antioxidant status of *Alternanthera brasiliana* against Ehrlich ascites carcinoma in Swiss albino mice. *Pharmacognosy Res*, **7**, 66.
- Sangameswaran B, Pawar Sunil P, Saluja Manmeet Singh SA, (2012). Antitumor activity of *Sida Veronicaefolia* against Ehrlich Ascites Carcinoma in mice. *J Pharm Res*, **5**, 315-9.
- Seong DB, Hong S, Muthusami S, et al (2016). Cordycepin increases radiosensitivity in cervical cancer cells by overriding or prolonging radiation-induced G2/M arrest. *Eur J Pharmacol*, **771**, 77-83.
- Sreelatha S, Padma PR, Umasankari E (2011). Evaluation of anticancer activity of ethanol extract of *Sesbaniagrandiflora* (Agati Sesban) against Ehrlich ascites carcinoma in Swiss albino mice. *J Ethnopharmacol*, **134**, 984-7.
- Stahmann MA, Graf LH, Patterson EL, Walker JC, Watson DW (1951). The inhibition of tobacco mosaic virus by synthetic lysine polypeptides. *J Biol Chem*, **189**, 45-52.
- Sunil D, Isloor AM, Shetty P, Nayak PG, Pai KSR (2013). In vivo anticancer and histopathology studies of Schiff bases on Ehrlich ascitic carcinoma cells: 1st cancer update. *Arab J Chem*, **6**, 25-33.
- Szende B, Szökán G, Tyihá E, et al (2002). Antitumor effect of lysine-isopeptides. *Cancer Cell Int*, **2**, 4.
- Torre LA, Bray F, Siegel RL, et al (2015). Global cancer statistics, 2012. *CA Cancer J Clin*, **65**, 87-108.
- Toshiyuki M, Reed JC (1995). Tumor suppressor p53 is a direct transcriptional activator of the human bax gene. *Cell*, **80**, 293-9.
- Wang D, Stockard CR, Harkins L, et al (2008). Immunohistochemistry in the evaluation of neovascularization in tumor xenografts. *Biotech Histochem*, **83**, 179-89.
- Watson DW, Bloom WL (1952). Antimicrobial activity of a natural and a synthetic polypeptide. *Proc Soc Exp Biol Med*, **81**, 29-33.
- Xie QJ, Cao XL, Bai L, et al (2014). Anti-tumor effects and apoptosis induction by Realgar bioleaching solution in Sarcoma-180 cells in vitro and transplanted tumors in mice in vivo. *Asian Pac J Cancer Prev*, **15**, 2883-8.
- Yip KW, Reed JC (2008). Bcl-2 family proteins and cancer. *Oncogene*, **27**, 6398-406.
- Zu K, Hawthorn L, Ip C (2005). Up-regulation of c-Jun-NH2-kinase pathway contributes to the induction of mitochondria-mediated apoptosis by α -tocopheryl succinate in human prostate cancer cells. *Mol Cancer Ther*, **4**, 43-50.